Electronic Supplementary Material (ESI) for Journal of Materials Chemistry A.

Supplementary Information

Carbon nanotube-induced phase and stability engineering: strained cobalt-doped WSe_2/MWNTs heterostructure for enhanced hydrogen evolution reaction

Guoyuan Zhang,[1,a] Xiaoli Zheng,[1,a] Qun Xu,*[,a] Jianan Zhang,[a] Wei Liu[a] and Jun Chen[b]

[a] College of Materials Science and Engineering, Zhengzhou University, Zhengzhou 450001, P.R. China

[b] ARC Centre of Excellence for Electromaterials Science, Intelligent Polymer Research Institute, Australian Institute of Innovative Materials, University of Wollongong, Wollongong, NSW 2500, Australia.

[1] These authors contributed equally to this work.

* Corresponding author, Email: qunxu@zzu.edu.cn

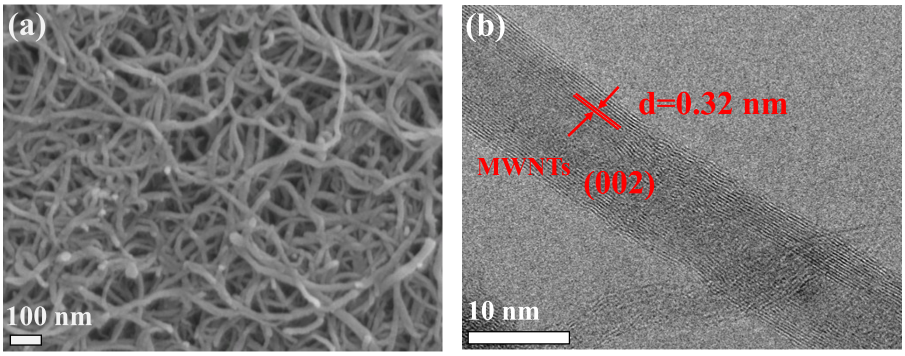

Figure S1. (a) SEM and (b) TEM images of pure MWNTs.

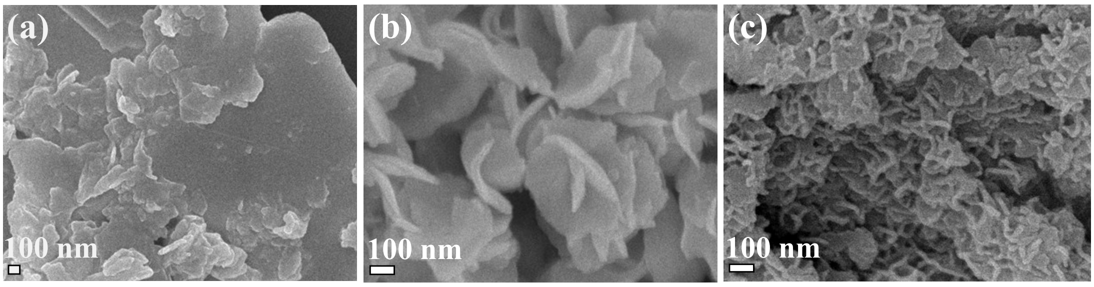

Figure S2. SEM images of (a) B-WSe_2, (b) WSe_2, (c) Co-WSe_2.

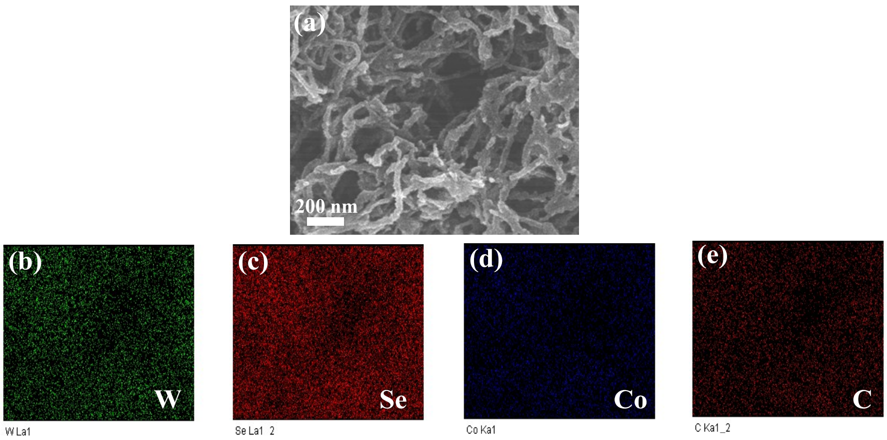

Figure S3. (a) SEM image and corresponding elemental mapping images of (b) W, (c) Se, (d) Co and (e) C of Co-WSe_2/MWNTs heterostructure, indicating the homogeneous dispersion of W, Se, and Co atoms around the whole MWNTs.

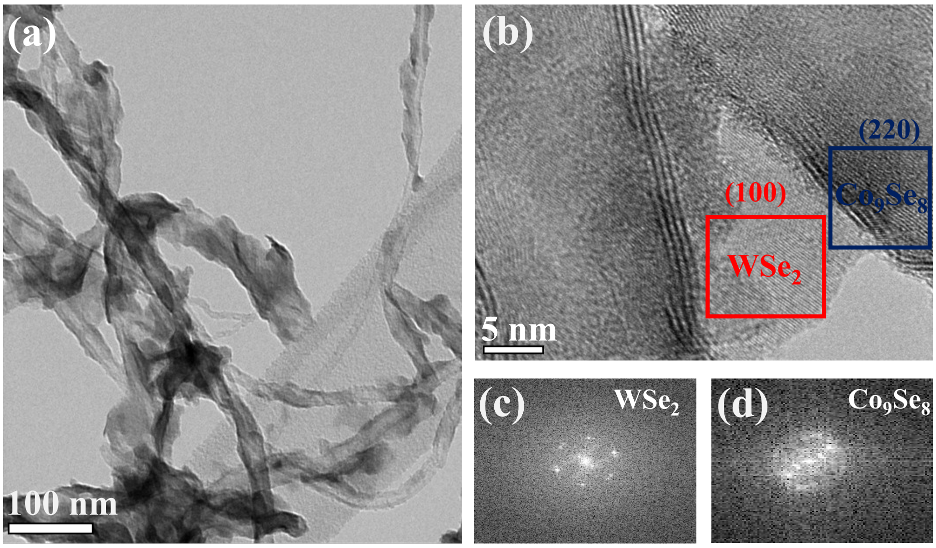

Figure S4. (a) TEM and (b) HRTEM images of Co-WSe_2/MWNTs, associated Fast Fourier Transform (FFT) of the region enclosed by the red square (c) and the blue square (d) in (b). The corresponding diffraction patterns clearly show the polycrystalline property of the Co-WSe_2 on the surface of MWNTs, showing that many defects are involved in the crystalline planes for increased active sites.

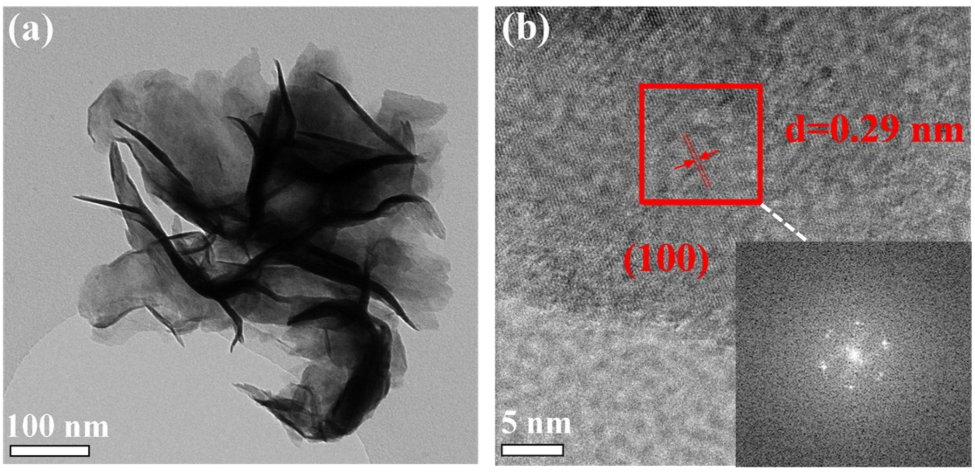

Figure S5. (a) TEM, (b) HRTEM images of WSe_2, the inset is the corresponding FFT image of the region enclosed by the red square in (b).

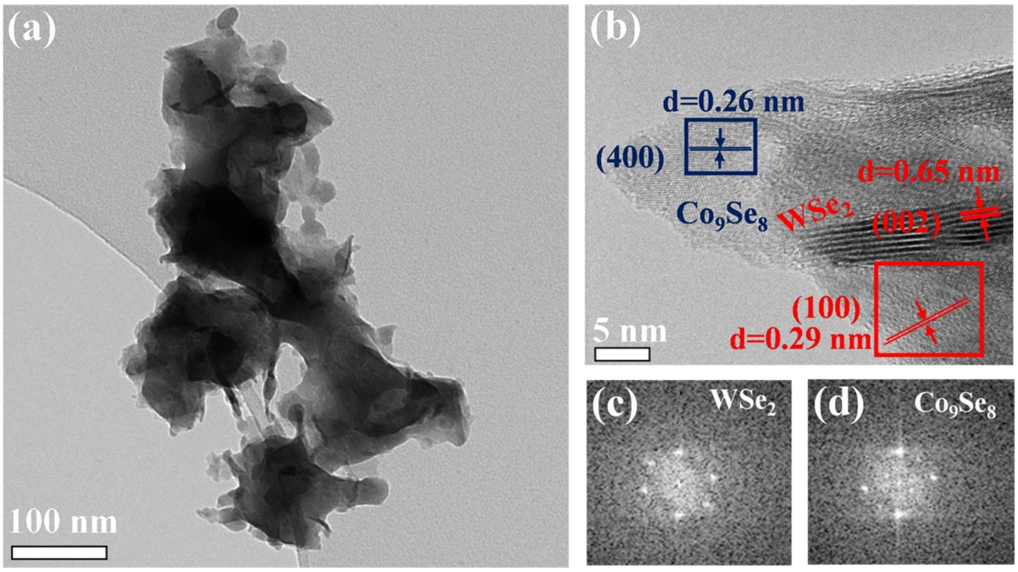

Figure S6. (a) TEM, (b) HRTEM images of Co-WSe_2, associated FFT of the region enclosed by (c) the red square of WSe_2, (d) the blue square of Co_9Se_8 in (b).

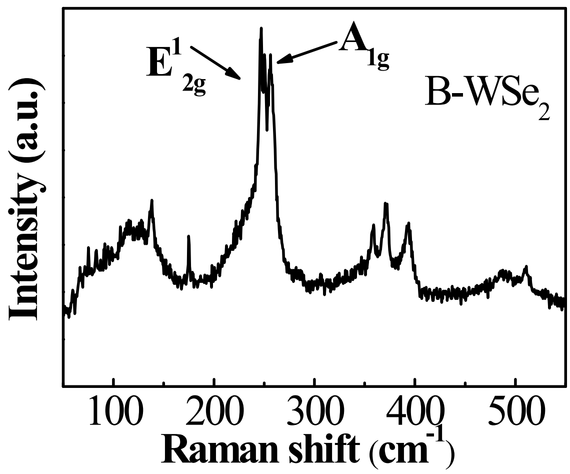

Figure S7. Raman spectrum of commercial B-WSe_2.

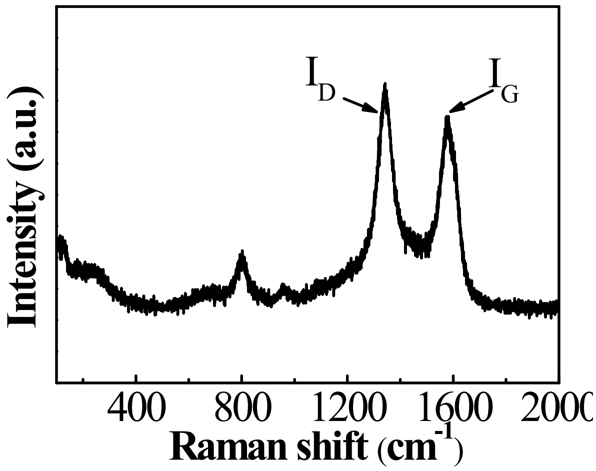

Figure S8. Raman spectrum of Co-WSe_2/MWNTs heterostructure in the range of 100-2000 cm^{-1}. The I_D/I_G intensity ratio can be calculated by the ratio of peak areas of D and G bands. The peak areas of D- and G- bands were obtained by fitting to the Lorentzian function with baseline corrections.

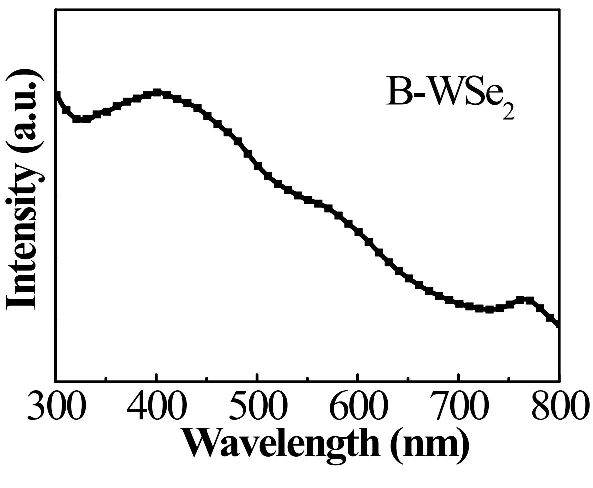

Figure S9. UV-vis absorption spectrum of commercial B-WSe_2.

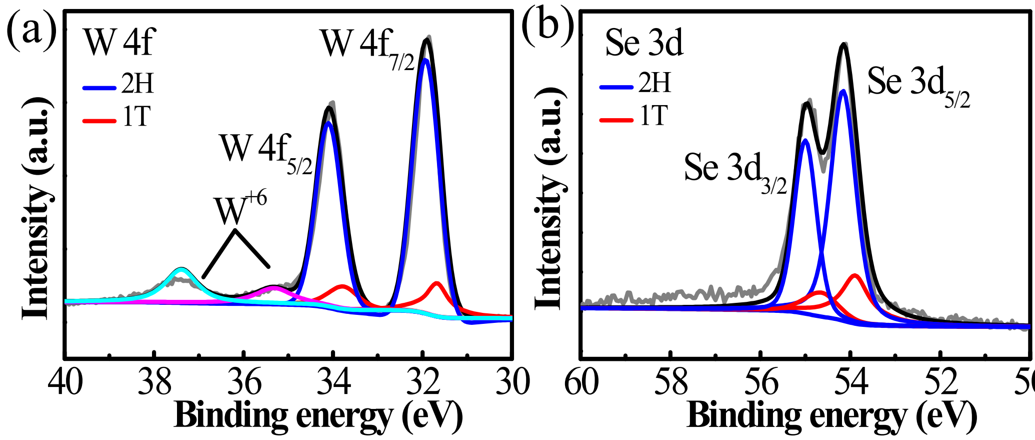

Figure S10. High resolution XPS spectra of (a) W 4f, (b) Se 3d of B-WSe_2. The curves are deconvoluted by Gaussian fitting.

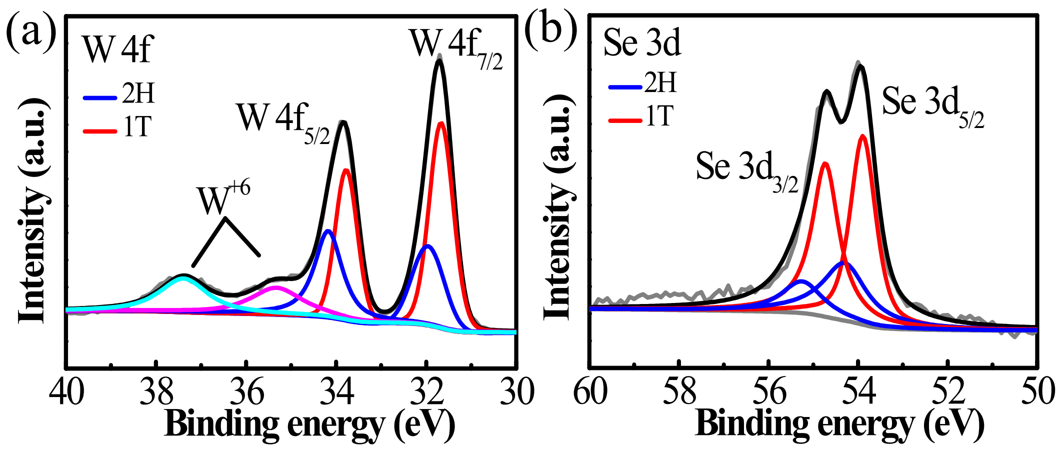

Figure S11. High resolution XPS spectra of (a) W 4f, (b) Se 3d of WSe_2. The curves are deconvoluted by Gaussian fitting.

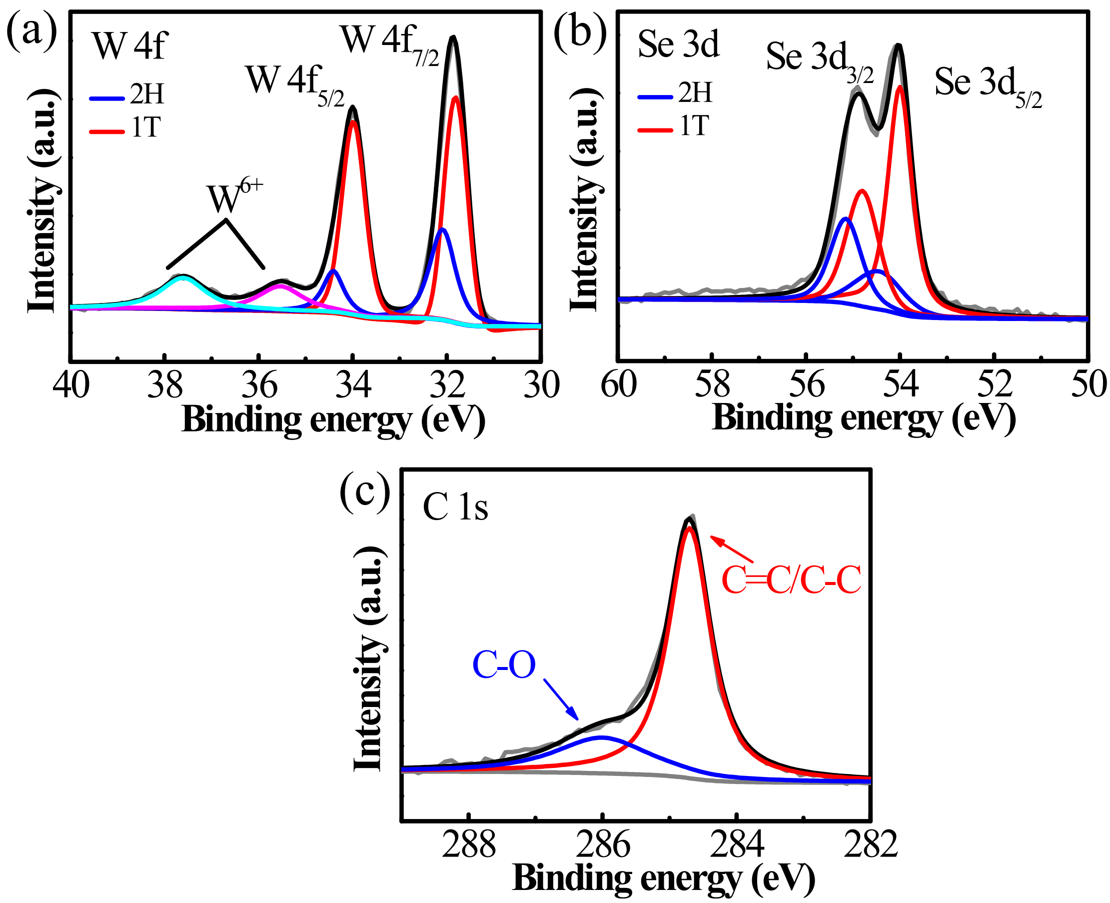

Figure S12. High resolution XPS spectra of (a) W 4f, (b) Se 3d, (c) C 1s of WSe_2/MWNTs. The curves are deconvoluted by Gaussian fitting.

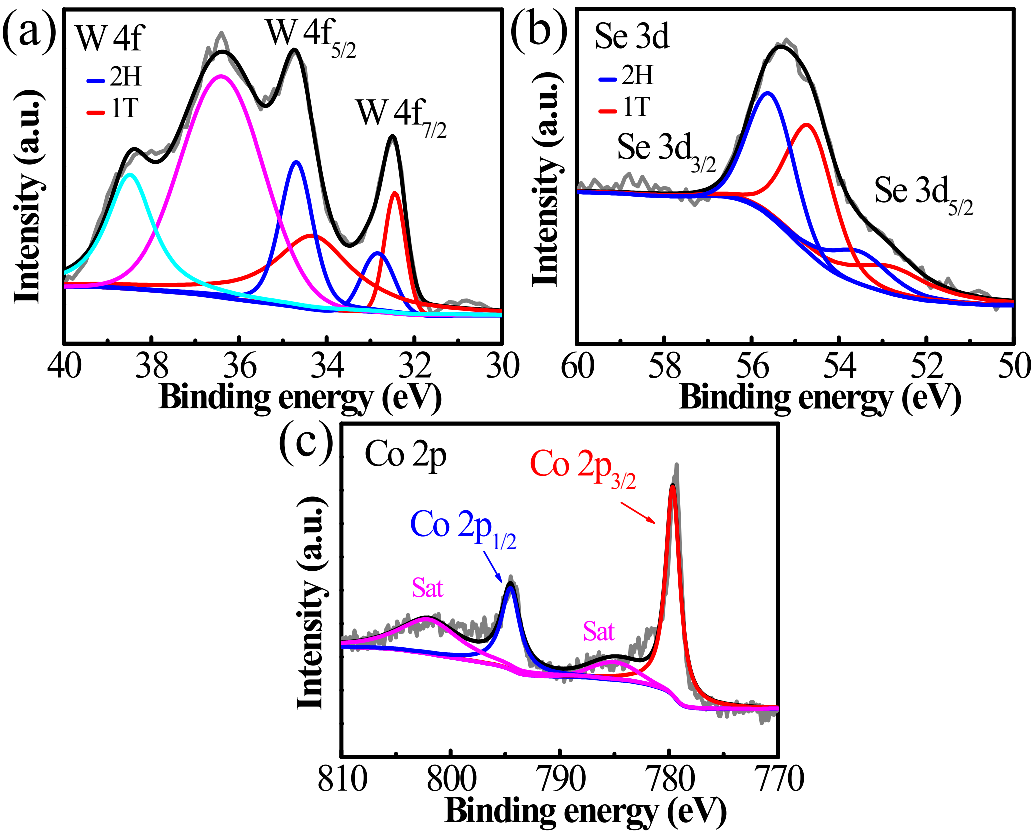

Figure S13. High resolution XPS spectra of (a) W 4f, (b) Se 3d, (c) Co 2p of Co-WSe_2. The curves are deconvoluted by Gaussian fitting.

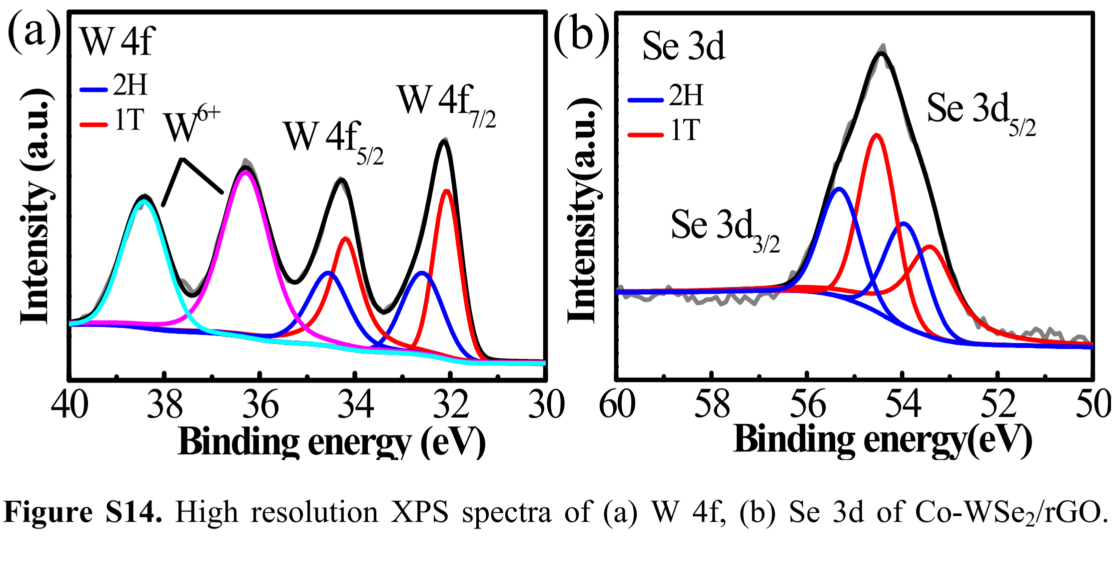

Figure S14. High resolution XPS spectra of (a) W 4f, (b) Se 3d of Co-WSe_2/rGO. The curves are deconvoluted by Gaussian fitting.

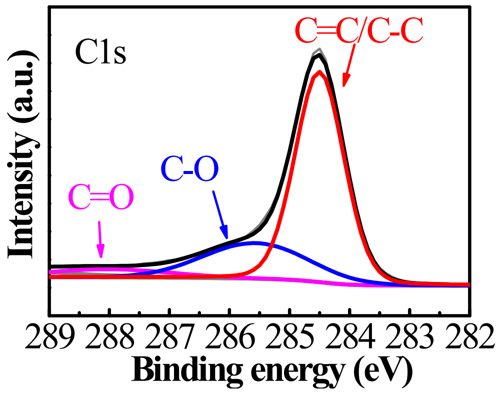

Figure S15. High resolution XPS spectrum of C1s of pristine MWNTs. The curves are deconvoluted by Gaussian fitting.

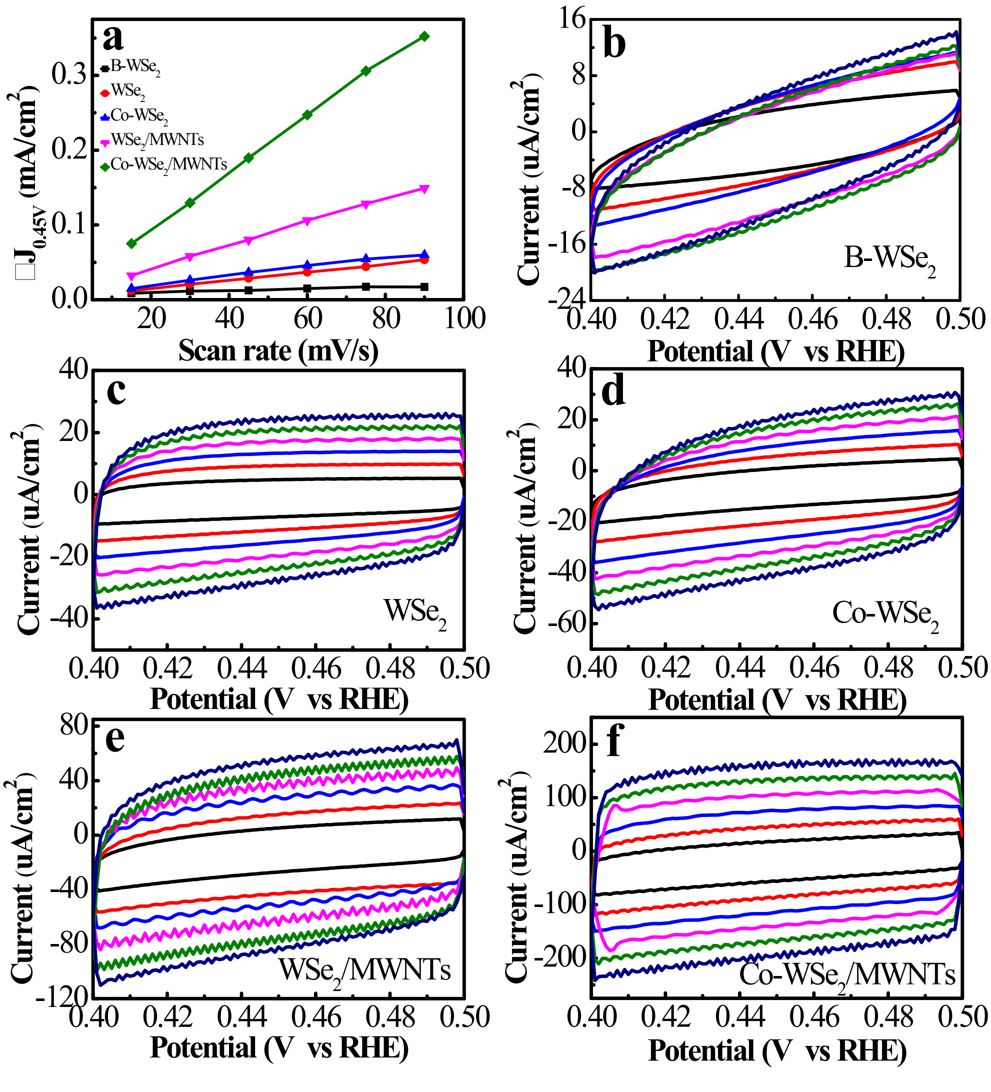

Figure S16. Capacitance measurements. (a) Relative electrochemically active surface area for the various samples, (b-f) cyclic voltammograms of B-WSe_2, WSe_2, Co-WSe_2,

WSe_2/MWNTs, and Co-WSe_2/MWNTs at various scan rates (15-90 mV S^{-1}) in the region of 0.4-0.5 V (vs RHE), in which no faradic processes are observed to obtain the capacitive current from double layer charging.

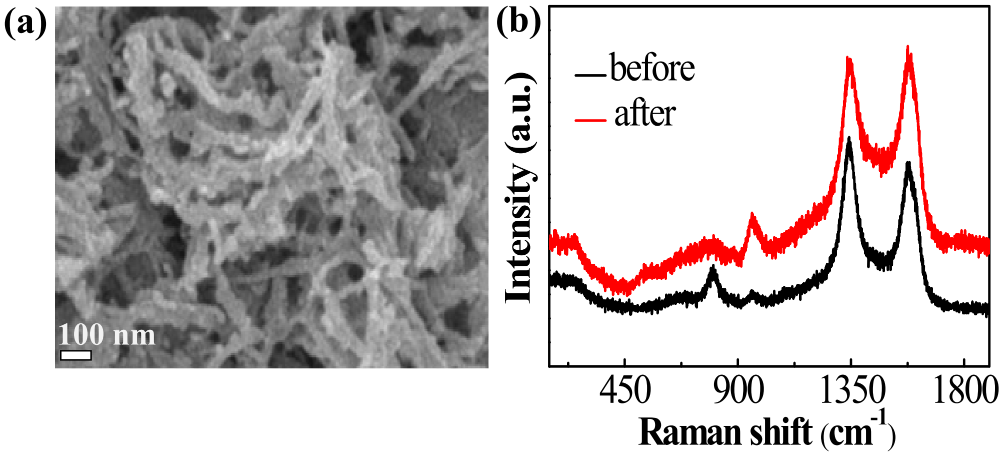

Figure S17. (a) SEM image and (b) Raman spectra for Co-WSe_2/MWNTs after 1000 cycles.

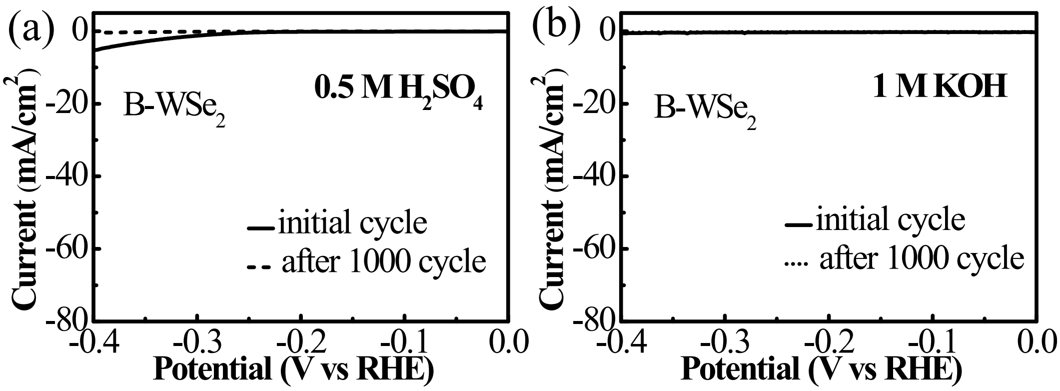

Figure S18. Durability test for B-WSe_2 in (a) 0.5 M H_2SO_4, (b) 1 M KOH after 1000 CV cycles storage under air atmosphere.

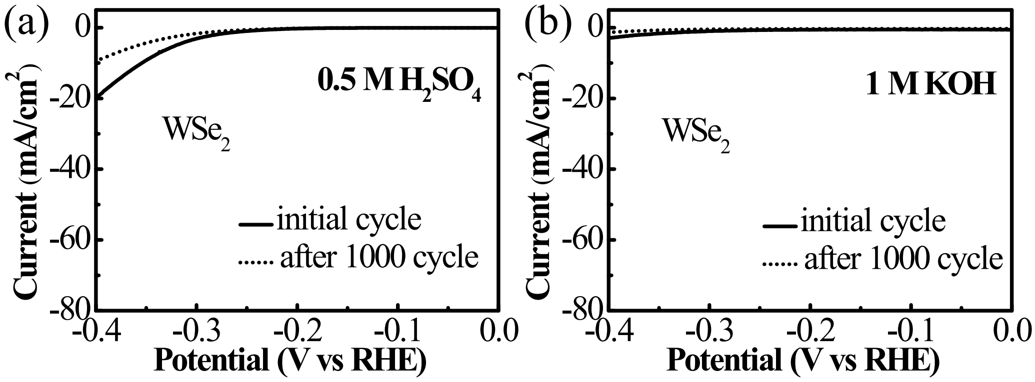

Figure S19. Durability test for WSe_2 in (a) 0.5 M H_2SO_4, (b) 1 M KOH after 1000 CV cycles storage under air atmosphere.

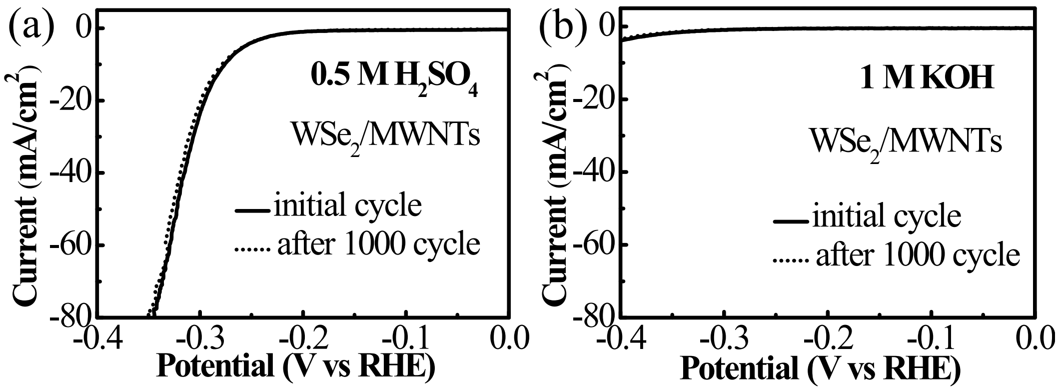

Figure S20. Durability test for WSe_2/MWNTs in (a) 0.5 M H_2SO_4, (b) 1 M KOH after 1000 CV cycles storage under air atmosphere.

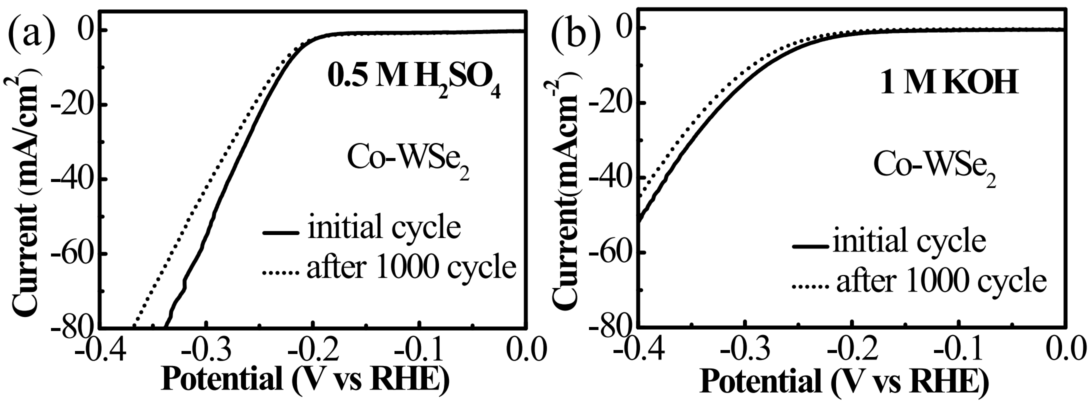

Figure S21. Durability test for Co-WSe_2 in (a) 0.5 M H_2SO_4, (b) 1 M KOH after 1000 CV cycles storage under air atmosphere.

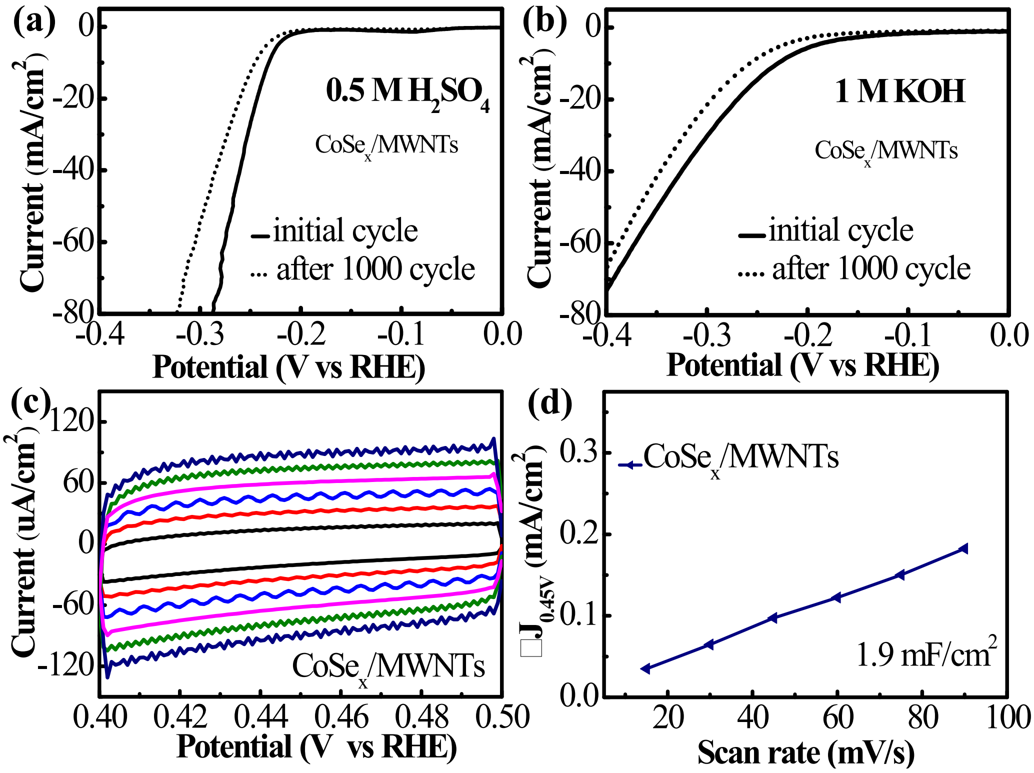

Figure S22. Electrochemical HER and durability measurements for $CoSe_x$/MWNTs in acidic solution (a) and alkaline solution (b), respectively. (c) Cyclic voltammograms of $CoSe_x$/MWNTs at various scan rates (15-90 mV S^{-1}) in the region of 0.4-0.5 V (vs RHE), in which no faradic processes are observed to obtain the capacitive current from double layer charging, (d) relative electrochemically active surface area.

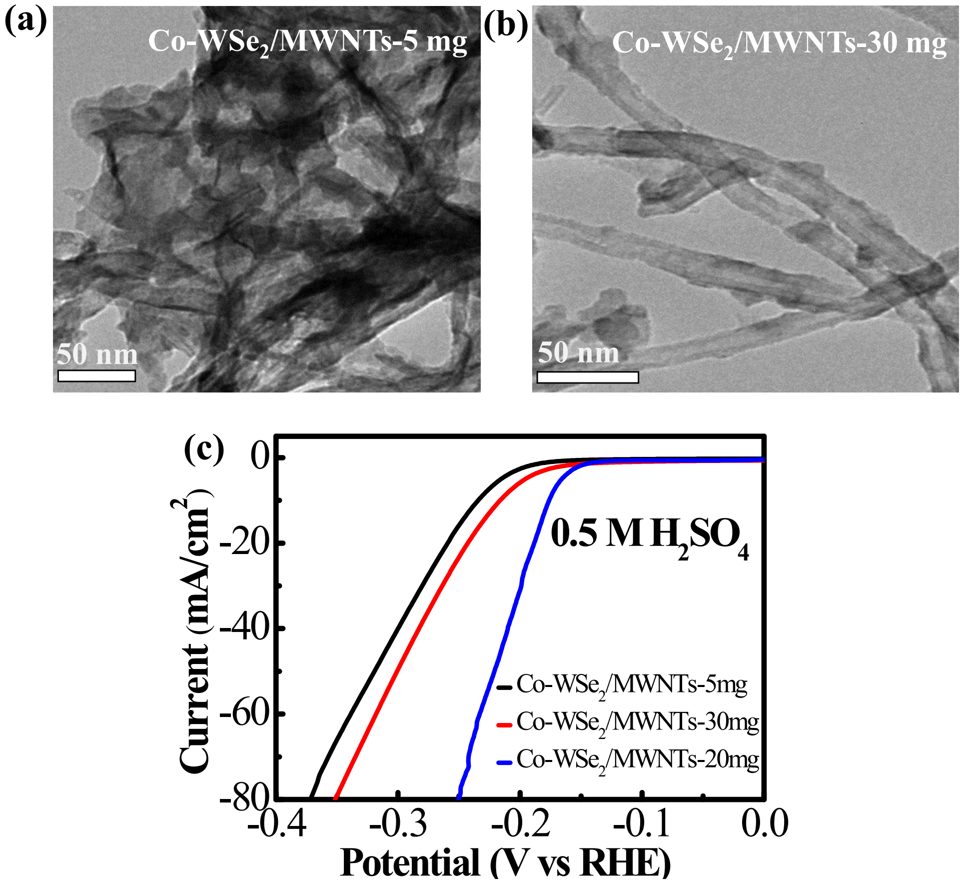

Figure S23. (a, b) TEM images and (c) HER measurements of Co-WSe_2/MWNTs heterostructures with different contents of MWNTs.

Table S1. Summary of the phase contents and oxidation degree of the samples.

Samples	Phase content (%)		Oxidation degree of W (%)
	2H	1T	
B-WSe_2	84.4	15.6	15.2
WSe_2	42.9	57.1	23.7
WSe_2/MWNTs	30.6	69.4	19.9
Co-WSe_2	40.0	60.0	58.6
Co-WSe_2/MWNTs	27.9	72.1	32.3
Co-WSe_2/rGO	41.3	58.7	48.2

Table S2. Electrocatalytic performance parameters of the samples in 0.5 M H_2SO_4.

Samples	η (vs RHE) at *j* = -10 mA cm^{-2} (mV)	Tafel slope (mV dec^{-1})	R_s (Ω) [a]	R_{ct} (Ω)	C_{dl} (mF)[b]
B-WSe_2	456	184	1.3	2103.0	0.1
WSe_2	353	93	1.4	6.8	0.5
WSe_2/MWNTs	275	68	1.4	6.2	1.6
Co-WSe_2	225	48	1.3	5.7	0.6
$CoSe_x$/MWNTs	232	41	1.4	5.9	1.9
Co-WSe_2/MWNTs	174	37	1.3	4.5	3.8

[a]The intercept of the semicircle on the real axis is assigned to the ohmic series resistance (R_s). [b] The C_{dl} of the catalysts can be investigated by cyclic voltammetry at various scan rates (Figure S16 and Figure S22).

Table S3. Comparison of electrocatalytic HER activity of the samples in this work with previously reported TMDs-based HER catalysts in 0.5 M H_2SO_4.

Catalyst	Tafel slope (mV dec^{-1})	η at 10 mA cm^{-2}	Charge-transfer resistance (R_{ct})	Ref.
WSe_2	93	353	6.8	This work
Co-WSe_2/MWNTs	37	174	4.5	This work
Exf-WSe_2	120	800	/	ACS Nano, 2014, 8, 12185
WSe_2	80	320	927	J. Mater. Chem. A, 2015, 3,12149
WSe_2/CNTs	59.7	228	258	
WSe_2	99	350	/	ACS Nano, 2014, 8, 8468
WSe_2 nanofilms on carbon fiber paper	77.4	300	/	Nano Lett. 2013,13, 3426
MoS_2 nanosheets	60	250	/	Nat. Mater. 2013, 12, 850

Table S4. Electrocatalytic performance parameters of the samples in 1M KOH.

Samples	η (vs RHE) at *j* = -10 mA cm^{-2} (mV)
B-WSe_2	581
WSe_2	485
WSe_2/MWNTs	458
Co-WSe_2	274
$CoSe_x$/MWNTs	230
Co-WSe_2/MWNTs	241